Removal of anionic dyes from aqueous solutions by cistus ladaniferus shells and their biochar: Isotherms, kinetic and thermodynamic studies

H. El Farissi[1], R. Lakhmiri[1*], A. Albourine[2], M. Safi[3] and O. Cherkaoui[4]

Abstract- The aim of this work is the valorization of the Cistus ladaniferus shells (CLSh) and the biochar of the Cistus ladaniferus shell (BCCLSh) as a bio-sorbent prepared by pyrolysis. Both adsorbents are characterized by scanning electron microscope (SEM), Fourier trans-form infrared spectroscopy (FTIR) and X-ray fluorescence (FX). The inexpensive, easy to obtain and environmentally friendly adsorbents has been used as an ideal alternative for dye removal methods in wastewater. CLSh and BCCLSh are two biomaterials used as bio-adsorbents for the removal of Reactive Red 23 (RR-23). The BCCLSh was prepared by pyrolysis under optimal conditions, at temperature of 450°C, a heating rate of 40°C.min^{-1} and particle sizes of 2 to 3 mm, the BCCLSh was then milled with a mill to a particle size of 0.1 to 0.2 mm. The adsorption kinetics of the dye by CLSh and BCCLSh are correctly described by the pseudo-second order model with a high correlation coefficient (R^2 = 0.997 for CLSh and 0.998 for BCCLSh). Experimental results showed that the adsorption isotherm models, Lungmuir and Freundlich are the two models suitable for BCCLSh with a correlation factor equal to 0.984 and for CLSh the adsorption isotherm is Lungmuir model type II. On the other hand the ability to remove the dye by BCCLSh is advantageous and the removal efficiency reaches a maximum value of 99.72% for BCCLSh and 93.32% for CLSh.

Index Terms - Bio-Char - Bio-Adsorbent - Cistus Shell - Pyrolysis - Eco-Friendly - Reactive Red 23.

1. INTRODUCTION

Wastewater Morocco has a large area of forests that provides a large biomass production for year for a various purposes (wood, firewood, charcoal production, pulp production, etc.). To that day, the use of cistus has been limited to the extraction of essential oils from these flowers. In studying the pyrolysis of cistus seeds and shells we have shown that those forest wastes materials are rich in carbon [1, 2].

- *H. El Farissi, Laboratory of Chemical Engineering and Valorization of the Resources, Faculty of Sciences and Techniques of Tangier, Abdelmalek Essaâdi University, Km 10 route de Ziaten, BP 416 Tangier, Morocco.*
- *R. Lakhmiri, Laboratory of Chemical Engineering and Valorization of the Resources, Faculty of Sciences and Techniques of Tangier, Abdelmalek Essaâdi University, Km 10 route de Ziaten, BP 416 Tangier, Morocco. PH- +212661427257 lakhmirir@yahoo.fr*
- *A. Albourine, Laboratory of Materials and Environment, Team of Coordination Chemistry, Faculty of Sciences, Ibn Zohr University, BP 8106, 80000 Agadir, Morocco.*
- M. Safi, *Laboratory of Physical Chemistry and Bio-Organic Chemistry, URAC University of Hassan II Mohammedia- Casablanca, Faculty of Sciences and Techniques-Mohammedia, BP 146,Mohammedia, Morocco.*
- *O. Cherkaoui, Laboratory REMTEX, Higher School of Textile and Clothing Industries, Casablanca, Morocco*

Adsorption has been recognized as a high efficiency process for the removal of dye onto activated carbon but it is an expensive process. For the valorization of those biomaterials (seeds and shell of cistus) which had never been studied in the adsorption of dyes in waste water treatment process, the CLSh and BCCLSh are two bio-materials may be used as bio-adsorbent for textile dyes. The reactive red 23 is one of the anionic dyes used for various purposes, wool, leather, jute, making red ink and printing on paper. The RR23 also affects the absorption and reflection of sunlight through the water, reduces solubility in oxygen and threatens the photosynthetic activity of aquatic plants and algae.

The effect in reducing oxygen levels interferes with the growth of bacteria so that they become ineffective in impurities biologically degrading in water and thus risk the food chain. These reasons make the effective removal of reactive dyes from textile industry effluents very important before entering the environment; Venkat S. Mane et al [3] has explored the adsorption characteristics of the Brilliant Green dye of the aqueous solution on sawdust treated with NaOH from eucalyptus wood. Removal of hazardous dye brilliant green from aqueous solution the reactive red 23 may form hazardous products like carbon oxides, nitrogen oxides, and sulfur oxides when heated to decomposition [4]. Various treatments

have been applied for the removal of synthetic dyes such as coagulation, flocculation, ion exchange, membrane filtration, photo-catalysis, and photooxidation. Adsorption and biosorption are known as an efficient and economic method for fading of dyes containing effluents. The major advantage of adsorption is the use of low-cost material, eco-friendly especially agricultural based biomass [5, 6.[

In our studies, the adsorption of the reactive red 23 on the seed of cistus ladaniferus and their biochar, the quantity eliminated in RR23 on the two materials is important, 62.5 mg.g-1 for CLS and 166.66 mg.g-1 for the BCCLS [7]. On the other hand, studies adsorption of the same dye on chitosan extracted from shrimp wastes were carried out [8]. Elimination of two dyes: Direct Red 23 and Acid Green 25, by chitosan in both systems single and binary were reported [9]. The adsorption study of the same dye (RR23) on the chitosan-silica (Si-Cs) composites in both Single and binary system shaw that the kinetic adsorption is of the second order and the ad-sorption isotherm in the Single system follows the model of Langmuir which gives the maximum adsorbed quantity equal to 128.2mg.g^{-1}, whereas in the binary system the adsorption isotherm follows the Freundlich model and the adsorbed quantity equal to 151.51mg.g^{-1} [10].

2. MATERIAL AND METHODS

2.1. The adsorbent

The CLSh and BCCLSh are two materials used for removal of the RR-23 dye; the BCCLSh is a pyrolysis product which is obtained under the optimum conditions, temperature equal 450 °C, particle size of 2 to 3 mm and heating rate equal to 40°C.min^{-1} [2]. The BCCLSh is then ground in a ceramic grinder until the particle sizes are between 0.1 and 0.2 mm.

2.2. Characterization of the Cistus Ladaniferus Shells and their biochar

The characterization of the CLSh and BCCLSh obtained under the optimal pyrolysis conditions was characterized by different technical of analysis. Fluorescence X-ray (table 1).

TABLE.1. *CHEMICAL ANALYSIS BY X-RAY FLUORESCENCE OF CLSh AND THE BCCLSh (CONTENT EXPRESSED IN% OF CONCENTRATION).*

Name of Compound	Weight %	
	Cistus Ladaniferus Shell (CLSh)	Biochar of Cistus Ladaniferus Shell (BCCLSh)
C	69.5	71.7
O	19.7	26.7
H	3.75	****
N	0.68	****
K	2.59	0.704
P	1.61	0.0423
Ca	0.824	0.383
Mg	0.705	0.0248
Na	0.178	0.0211
Fe	0.1701	0.04
Cl	0.146	0.175
Si	0.101	0.0633
S	0.006	****
Mn	0.059	0.0157
Al	0.045	0.0167
Zn	0.0249	0.0112
Cu	0.0159	0.0105
I	0.0077	0.0071
Ni	0.00705	****
Rb	0.0029	****

SEM analysis allows microscopic characterization of the CLSh and BCCLSh contact surface by means of an SH-4000M apparatus. (Figure 1) shows the results obtained by SEM on particles (0.1 - 0.2 mm in size) of BCCLSh and the (figure 2) shows the results SEM of CLSh.

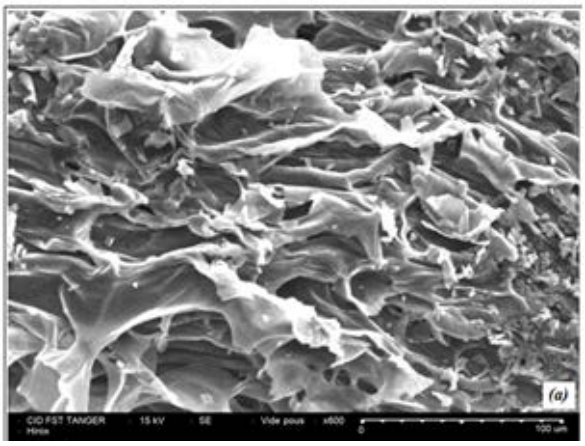

Fig.1. (a) *Micrographs (15kv, G*600) of BCCLSh*

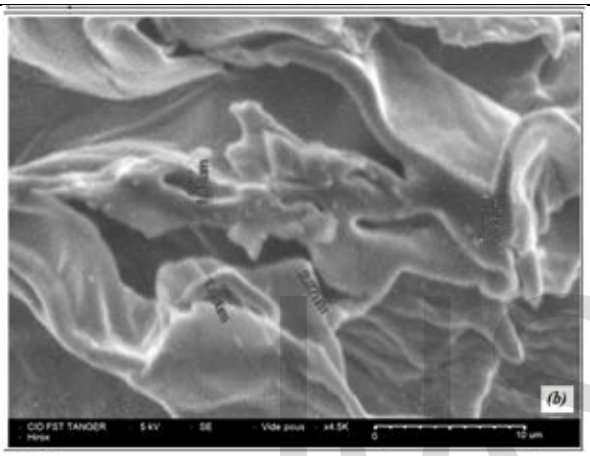

Fig.1. (b) *Micrographs (5kv, G*4500)[(b)] of BCCLSh*

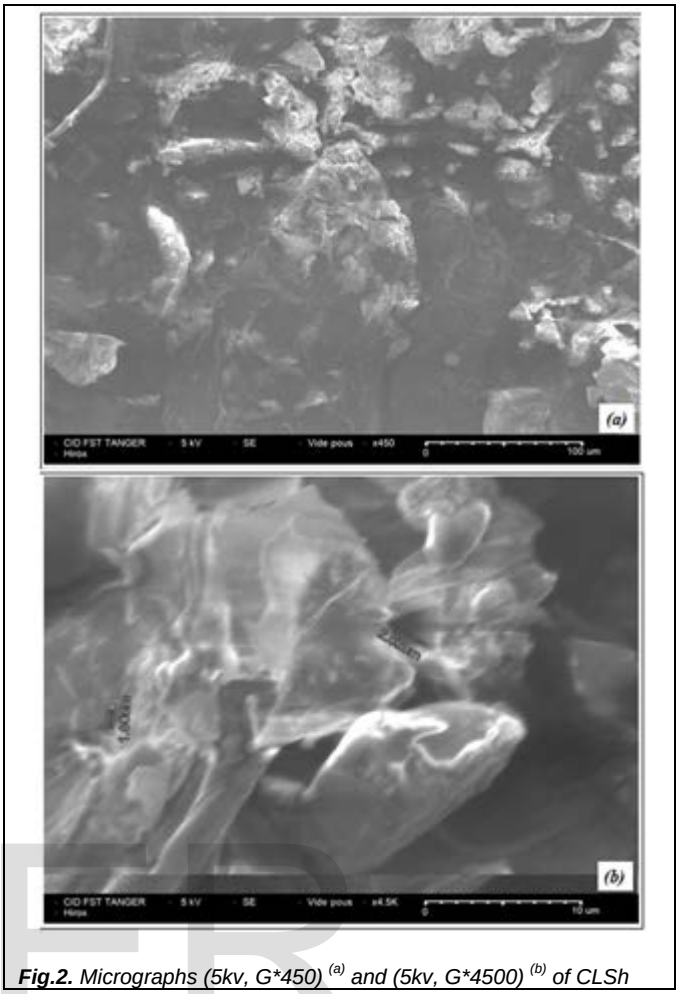

Fig.2. *Micrographs (5kv, G*450) [(a)] and (5kv, G*4500) [(b)] of CLSh*

The EDXA spectrum of CLSh and BCCLSh (figure 3 (a) and (b)) also confirms the presence of a high percentage of carbon and oxygen in the two materials. The micrographic image of BCCLSh and CLSh are shown in figure 1 and 2 respectively, which giving a clear idea on the morphology of materials by the presence of mi-cropores and nano-pores which favors the adsorption of RR-23 of the two materials.

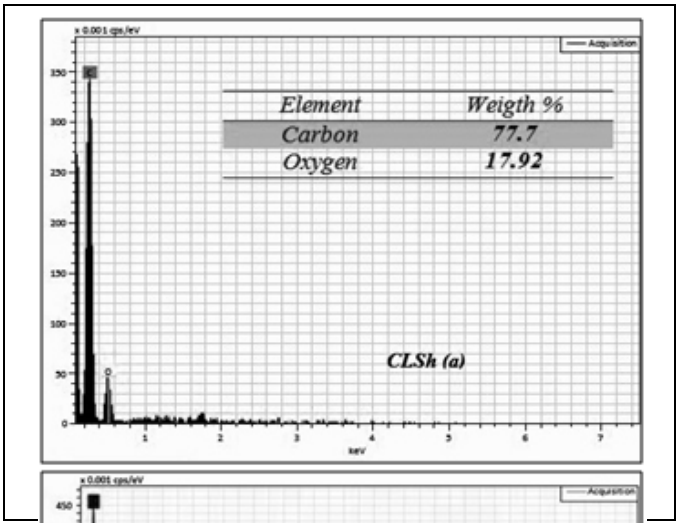

Fig.3. *EDXA spectra of CLSh (a) and BCCLSh (b)*

Fourier transform infrared spectroscopy (FTIR) reveals the chemical groupings present in the CLSh and BCCLSh. Figure 4 shows the cistus seeds and their bio-char FTIR spectrum.

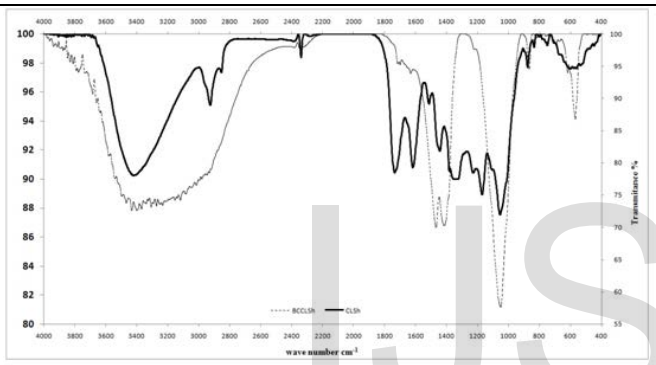

Fig.4. *FTIR spectrum of the CLSh and their BCCLSh*

The FTIR spectrum in (figure 4), of CLSh and BCCLSh shows the presence of -OH groups of the first and secondary alcohols and phenols between 3000 to 3650cm^{-1}. This is confirmed by the presence of the antisymetric vibrations of the -CH2 to 2925cm^{-1}, -OH bonds free at 3670cm^{-1}. The presence of phosphines with poor peaks between 2280 to 2410cm^{-1}, C=O esters (lactams at four centers) between 1720 to1765 cm^{-1}, aromatic amines at 1515 cm^{-1}, isopropyl group $(CH_3)_2CH$- bonds between 990 to 1050 cm^{-1}, C-N bonds of the nitrile derivatives at 834 cm^{-1}, Ar-OH bonds at 602 cm^{-1}, nitriles between 530 to 580 cm^{-1}, C-C-C-N bonds of the cyclanes between 430 to 580cm^{-1}. On the other hand, the isopropyl bonds disappeared in BCCLSh. The same re-mark applies for the free -OH group which are converted to –NH bonds of the primary and secondary amines thus the percentage of oxygen deprived also.

2.3. Adsorbate RR-23

The anionic dye used in this study is the reactive red 23.The dye stock solution was prepared by dissolving 0.12 g of RR-23 in 1L of distilled water and the required concentration of the working dye solution was prepared by diluting the stock solution with water distilled.

TABLE 2

PHYSICOCHEMICAL CHARACTERISTICS OF THE RR-23DYE

Usual name	Reactive Red 23 (RR-23)
Chemical formula	$C_{18}H_{13}N_2Na_3O_{14}S_4$
Molecular weight	678.53 g.mol^{-1}
Solubility in water	High
λ_{max} (nm)	511

2.4 Adsorption Process

2.4.1 Adsorption kinetics.

The adsorption kinetics are studied on the CLSh and BCCLSh, operating under optimum conditions (pH = 7 ± 0.5, adsorbent dose = 50 mg, dye concentration 50mg.L^{-1}, stirring speed = 200tr.min^{-1}). In Erlenmeyer rode, 50 mg of the adsorbent are mixed with 50 ml of the RR-23 solution (C_0 =50mg.L^{-1}). The suspension is stirred at 200tr.min^{-1} at room temperature (25 ±1°C). At defined time intervals ranging from 15 to 180 min, the cistus seeds and their bio-char are separated from the liquid by centrifugation. The concentration of the RR-23 in the liquid phase is then determined by measuring the absorbance at 511 nm and reading on a calibration curve established from a range of RR-23 concentrations ranging from 0.0 to 45mg.L^{-1}. The amount of RR-23 (Q_t) adsorbed by cistus seeds and their bio-char as a function of time are calculated according to the following formula:

$$Q_e = \frac{(C_0 - C_e)*V}{m} \quad \text{(eq.1)} \qquad R\% = \frac{(C_0 - C_e)}{C_0} * 100 \quad \text{(eq.2)}$$

C_0: concentration initial dye in (mg.L^{-1}); C_e: final dye concentration in solution (mg.L^{-1}); V: volume of the dye solution in L; m: mass of cistus seed or bio-char of cistus seed in g; R%: Removal; Q_e: Amount adsorbed in (mg.g^{-1})

The four models tested for the adsorption kinetics of the RR-23 dye by cistus seeds and their bio-char are presented below.

- Pseudo-first-order:

In 1898, Lagergren [11] proposed a pseudo-first-order equation in order to clarify the adsorption of the liquid / solid system. On the basis of this equation, the velocity of change for sorbate uptake with time is directly

proportionate to the difference in the saturation concentration and the amount of solid uptake with time. Pseudo-first-order equation represented by below equation [10]:

$$\frac{dq_t}{dt} = k_1(q_e - q_t) \text{ (eq.3)}$$

Where q_e: the dye amount adsorbed at equilibrium (mg.g^{-1}), q_t: the dye amount adsorbed at time t (mg.g^{-1}) and k_1: the equilibrium rate constant of pseudo-first-order kinetics (1/min) and t: contact time (min).

After integration by applying conditions, q_t=0 at t=0, then equation (eq-3) becomes:

$$Q_t = Q_t\left(1 - e^{-k_1 t}\right) \text{ (eq.4)}$$

The linearization of the previous equation gives

$$Ln(Q_e - Q_t) = -K_1 t + Ln\, Q_e \text{ (eq.5)}$$

Where Q_e and Q_t are the amounts (mg.g^{-1}) of the adsorbed RR-23 at equilibrium and time t respectively; K_1 is the adsorption rate constant (mL.min^{-1}). The constants of the model are determined graphically by plotting ($\ln(Q_e-Q_t)$) as a function of t.

- Pseudo-2ndorder model is given by the following expression [12]:

$$\frac{dq_t}{dt} = k_2(q_e - q_t)^2 \text{ (eq.6)}$$

After integration by applying conditions, q_t=0 at t=0, then equation (eq-6) and the linearization of the previous equation gives

$$\frac{t}{Q_t} = \frac{t}{Q_e} + \frac{1}{K_2 Q_e^2} \text{ (eq.7)}$$

Where, K_2 (g.mg^{-1}.min) is the adsorption rate constant. The constants (K_2 and Q_e) are also determined graphically by plotting (t/Q_t) as a function of t.

- The Elovich model can be expressed by the equation [13].

$$\frac{dq_t}{dt} = \alpha\, e^{-\beta q_t} \text{ (eq.8)}$$

To simplify the Elovich equation it was supposed that $\alpha\ \beta\ t >> 1$ and that q_t=0 with t= 0, therefore one obtains:

$$Q_e = \frac{1}{\beta} Ln\, t + \frac{1}{\beta} Ln\,(\alpha\beta) \text{ (eq.9)}$$

α is the initial adsorption capacity (mg.g^{-1}.min) and β is the desorption constant (g.mg^{-1}). The curve of Q_t as a function of ln (t) gives a regression line with a slope corresponding to ($1/\beta$) and an ordinate at the origin giving the term ($1/\beta$)ln ($\alpha\beta$).

- Intraparticule Diffusion model [13]:

$$Q_e = K_i \sqrt{t} + C \text{ (eq.10)}$$

Where, K_i is the intraparticule diffusion rate constant. The value of the ordinate at the origin C provides an indication of the thickness of the boundary layer.

2.4.3 Obtaining and modeling of the adsorption isotherm.

To obtain the adsorption isotherm, a serie of Erlenmeyers is used. In each Erlenmeyer are poured 50 ml of RR-23 solution dye of varying concentrations: 0; 10; 20; 30; 40; 50; 60; 70; 80; 90 and 100 mg.L^{-1}. The adsorption equilibrium study is carried out under the same optimum conditions indicated above. After equilibration, the particles of the adsorbent are separated by centrifugation and the clarified solution is analyzed by determination of the equilibrium concentration (C_e) of RR-23 using the same calibration curve used previously. The quantity of the adsorbed reagent at equilibrium (Q_e, in mg.g^{-1}) is calculated by equation (eq-1).

The following four conventional models, in their linear forms, are used to describe the adsorption isotherms:

- The Lungmuir model [15]:

$$Q_e = \frac{Q_m K_L C_e}{1 + K_L C_e} \text{ (eq.11)}$$

This equation can be reshaped and rearranged into linear of the following equations [16].

$$\frac{C_e}{Q_e} = \frac{C_e}{Q_m} + \frac{1}{Q_m K_L} \text{ (eq.12)}$$

Q_e is the amount (mg.g^{-1}) of RR-23 adsorbed at equilibrium; this is the equilibrium concentration (mg.L^{-1}); Q_0: the monolayer adsorption capacity (mg.g^{-1}); K_L: the Lungmuir constant (L.mg^{-1}) related to the adsorption free energy.

An essential characteristic of the Lungmuir isotherm can be expressed in terms of a dimensionless constant called the separation factor and defined by the equation below[17].

$$R_L = \frac{1}{1 + K_L C_0} \text{ (eq.13)}$$

Where C_0 is the initial concentration of the adsorbate (mg.L^{-1}) and K_L is the Lungmuir constant (L.mg^{-1}). A separation factor R_L> 1 indicates that the adsorption is unfavorable, if R_L = 1 the adsorption is said to be linear, adsorption is said to be favorable when 0 <R_L <1, and a zero separation factor (R_L = 0) Indicates that adsorption is irreversible. In our case, the found values of R_L are all between 0 and 1, which reveals favorable adsorption.

- The Freundlich equation:

The Freundlich isotherm was used for heterogeneous sorption and to describe the adsorption of organic and inorganic components in the solution [18]. The Freundlich isotherm has a linear expression, as shown by eq.14.

$$Ln\, Q_e = \frac{1}{n} Ln\, C_e + Ln\, K_F \text{ (eq.14)}$$

K_F is a constant indicating the relative adsorption capacity of the adsorbent (mg.g^{-1}) and 1/n indicates the adsorption intensity. These constants are determined from the equation of the line ($Ln\, Q_e$) = f(LnC_e).

- The Temkin equation [19]:

$$Q_e = \frac{RT}{b} Ln\, C_e + \frac{RT}{b} Ln\, K_T \text{ (eq.15)}$$

Where T: absolute temperature in °K, R: perfect gas constant (8.314 J.mol^{-1}.K^{-1}), B_1 (J.mol^{-1}): adsorption heat; K_T

($L.mg^{-1}$): constant corresponding to the maximum equilibrium binding energy.

- The equation of Dubinin-Radushkevich [20]

$$\text{Ln } Q_e = -K_D \varepsilon^2 + \text{Ln } Q_m \quad \text{(eq.16)}$$

□: the potential of Polanyi, corresponding to:

$$\varepsilon = RT\text{Ln}\left(1 + \frac{1}{C_e}\right) \quad \text{(eq.17)}$$

And K_D: the adsorption constant per molecule of the adsorbate when it is transferred to the surface of the solid from the infinite in the solution[21]. K_D and E ($KJ.mol^{-1}$) are linked by the relationship

$$E = \frac{1}{\sqrt{2K_D}} \quad \text{(eq.18)}$$

3. RESULTS AND DISCUSSION

3.1 Effect of various parameters on the elimination of RR-23

3.1.1 Effects of pH on removal of RR-23

The effect of pH on the removal of RR-23 using a CLSh and the BCCLSh are shown in Figure 5.

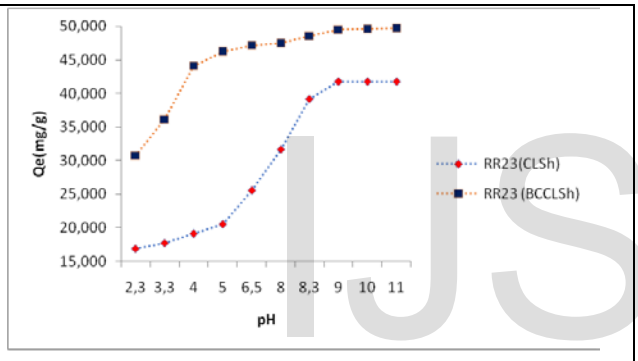

Fig.5. *The effect of pH on the adsorption of RR-23 dye on the CLSh and BCCLSh. (t=90 min; T=25±1°C, Initial dye Co =50mg.L^{-1}; Adsorbent mass=50mg; Stirring=200 rpm).*

The effect of pH on the adsorbed amount is very important for both adsorbents. The adsorbed amount per CLSh is observed to vary slightly from 16.89 to 20.5mg.g^{-1} when the pH is increased from 2.3 to 5. This low variation due to the formation of the binding bonds, the adsorbent quantity varies very rapidly from 30.76 to 46.17mg.g^{-1} at the same pH, hence the variation from to the form of charcoal which is very porous and has the structure which is formed by well-organized leaves. When the pH increases from 5 to 8.3 the adsorbed amount varies very rapidly for CLSh, while the amount adsorbed by BCCLSh increases from 46.17 to 48.55mg.g^{-1} and for CLSh from 20.5 to 39.17mg.g^{-1}. This important variation may be due to the decrease of the H^+ protons on the surface and the increase of the HO^- ions which favors the adsorption by release of the active sites in the adsorbate. Finally, for pH between 8.3 and 11, the adsorbed quantity remains almost fixed for the two adsorbates with a rate of variation not exceeding 0.03mg.g^{-1} for CLSh and 0.1mg.g^{-1} for BCCLSh.

3.1.2 Effects of dose adsorbent on removal of dye.

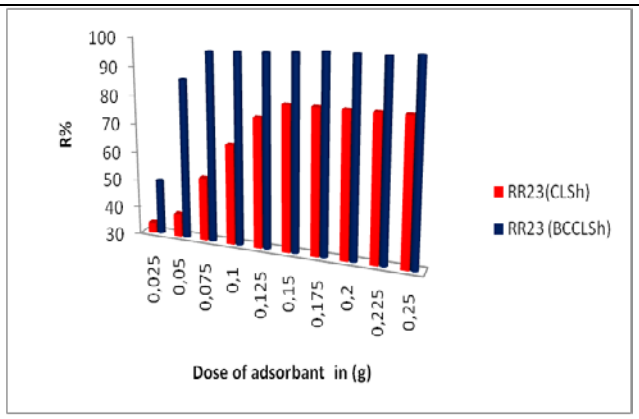

Fig.6. *Effect of CLSh or BCCLSh amount on the adsorption of RR23dye, (t =90min, T=25±1°C, Co=50mg.L^{-1}, Stirring 200rpm and pH=7±0.5)*

The figure 6 shows the variation of RR-23 dye removal efficiency by CLSh and BCCLSh. When, the mass varies from 25mg to 150mg, the yield of removal dye is increases from 33.62 to 80.75% for CLSh and from 49.43 to 97.82% for BCCLSh. For mass ranging from 175mg to 250mg the dye removal efficiency varies from 98.72 to 99.58% for the BCCLSh and 80.88 to 80.99% for the CLSh. We can conclude that when the mass of adsorbate is larger the dye removal does not evolve, so we will have the equilibrium between the adsorbate and adsorbent or graduations of the concentration.

3.1.3 Effect of initial concentration on removal of dye

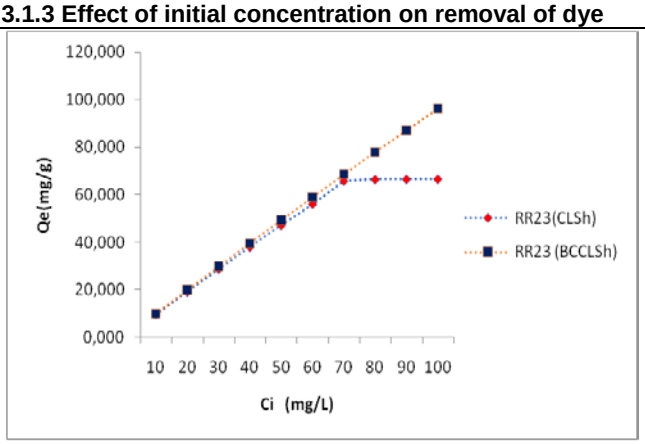

Fig.7. *Effect of initial dye concentration on BCCLSh and CLSh adsorption (t=90min, T=25±1 °C, Stirring = 200rpm and pH=7±0.5)*

The effect of the initial concentration of RR-23 in the range from 10 to100 mg.L^{-1} on the percentage removal and uptake of RR-23 dye by CLSh and BCCLSh was investigated under experimental conditions, the results are shown in Figure 7 at dye concentrations below 60mg.L^{-1}, the ratio of RR-23 to the vacant sites of CLSh or

BCCLSh is high, resulting in increased dye removal and the transfer to the absorbing surface by migration and convection. At higher dye concentrations, the lower percentage of elimination is due to saturation of the active sites for CLSh, or to a possible repelling force between the adsorbed layers and the remaining bulk molecules. The data show that absorption of RR-23 by BCCLSh increases from 9.97 to 96.37mg.g^{-1} and the percentage of elimination of RR-23 decreases from 99.72 to 96.37% with increasing the dye concentration from 10 to 100mg.L^{-1} respectively. On the other hand, for CLSh, the percentage of elimination of RR-23 decreased from 96.28 to 93.89% with an increase in the dye concentration of 10 to 70 mg.L^{-1} respectively and for a concentration ranging from 70 to 100mg.L^{-1} the percentage of elimination follows their emission up to 66.54% in particular the quantity adsorbed remains almost constant varies from 65.73 to 66.54mg.g^{-1}. In fact, the increase of the concentration induces an increase of the driving force of the concentration gradient, thereby increasing the diffusion of the dye molecules in solution across the surface of the adsorbent.

3.1.4 The effect of contact time

Figure 8 shows the change in the adsorbed amount of the RR-23 dye per gram of CLSh or BCCLSh as a function of the contact time at an initial dye concentration set at 50mg.L^{-1}. The adsorbed amount varies very rapidly from 34.05 to 49.43mg.g^{-1} for BCCLSh and from 18.95 to 34.93mg.g^{-1} for CLSh when the contact time increases from 10 to 50 min. it can be deduced that the selectivity of BCCLSh is greater than that of CLSh. For a contact time ranging from 60 to 120 min, the amount adsorbed by CLSh increases from 35.23 to 35.33 mg.g^{-1} and for BCCLSh increases from 49.45 to 49.75 mg.g^{-1} respectively.

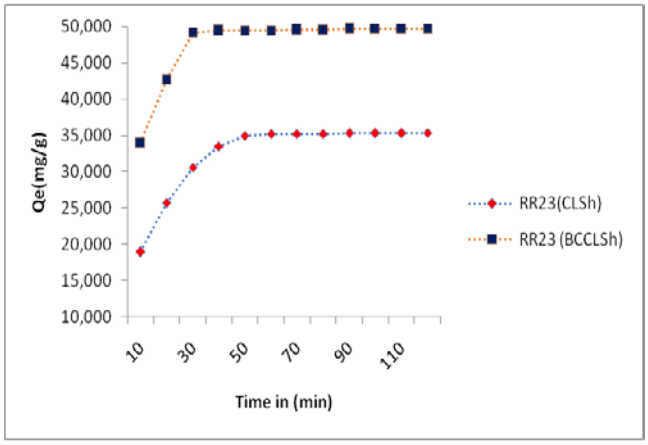

Fig.8. *Effect of contact time on dye adsorption on CLSh and BCCLSh (T=25±1°C, C_0 = 50mg.L^{-1}, Stirring = 200 rpm and pH=7± 0.5)*

3.1.5 The effect of temperature

The figure 9 show the temperature has a negative effect on the adsorption, that a decrease in the amount adsorbed by the two adsorbates is observed when the temperature increases by 25°C to 75°C. The amount adsorbed by CLSh and BCCLSh increased from 46.99 to 29.46mg.g^{-1} and from 49.42 to 41.90mg.g^{-1} respectively.

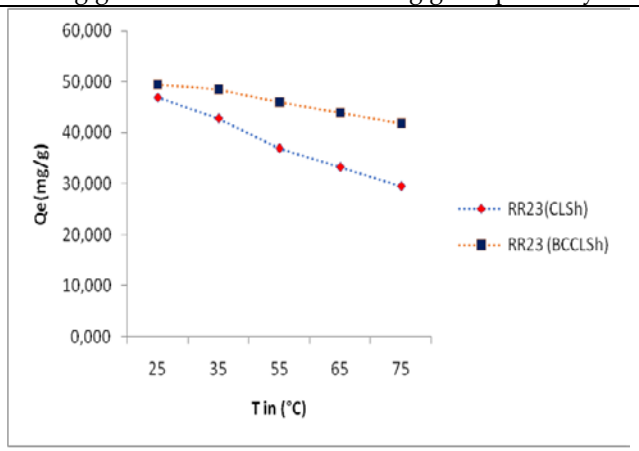

Fig.9. *Effect of temperature on dye adsorption on CLSh and BCCLSh (T=25±1°C, C_0 = 50mg.L^{-1}, Stirring = 200 rpm and pH =7± 0.5)*

3.2 Adsorption Kinetics

The four models of the kinetics tested are presented in Figure 10.

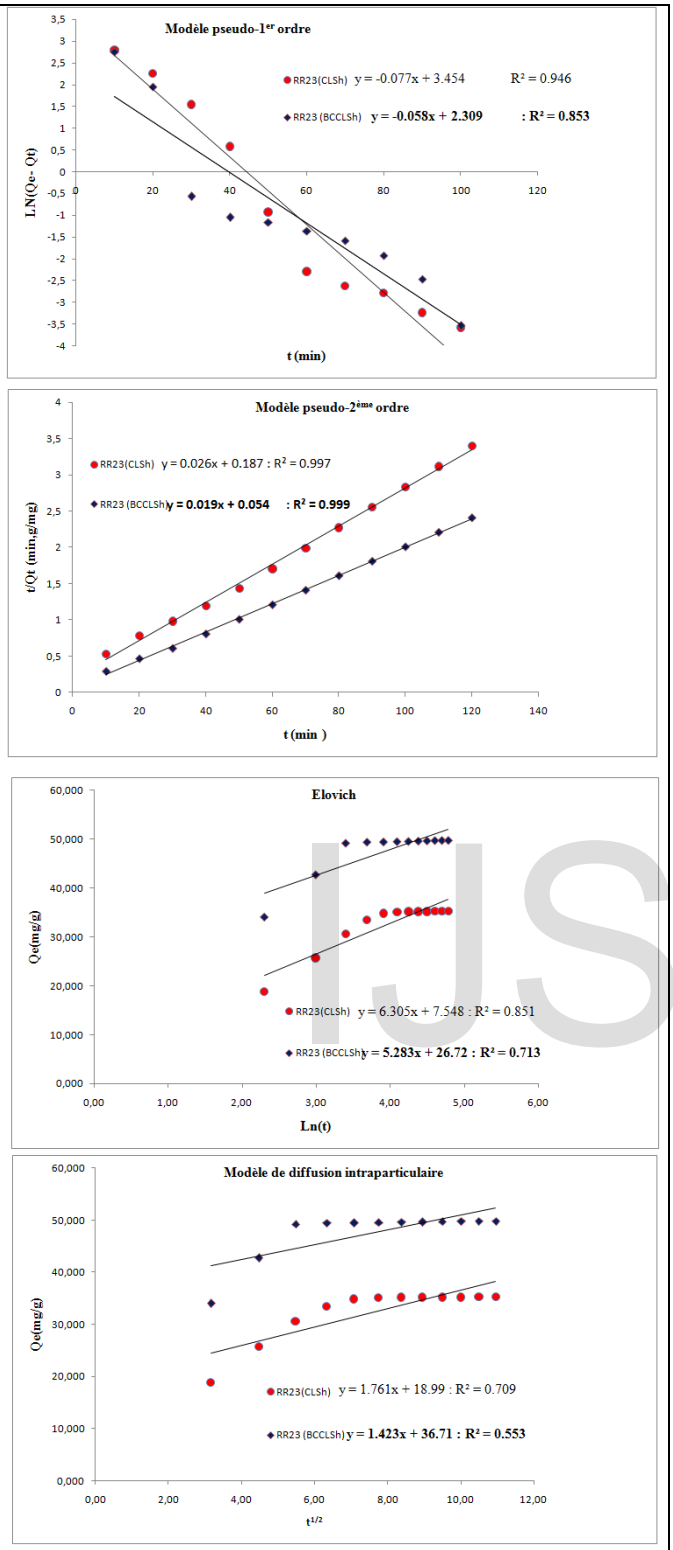

Fig.10.*The four kinetic model of dye adsorption on CLSh and the BCCLSh (T=25±1°C, m =50mg, C_o=50mg.L^{-1}; stirring =200 rpm and pH=7±0.5)*

The choice of the best model established for the study of the adsorption kinetics is selected as a function of the correlation factor. From the results of Figure 10 and Table 3, we find that the model with the highest correlation factor is the pseudo-second order model (R^2 = 0.997 for CLSh and R^2=0.999 for BCCLSh), we can deduce that the pseudo-second order is that which describes the adsorption process of the RR23 dye on the CLSh and the BCCLSh, we also see that the adsorbed quantities calculate $Q_{e,cal}$ by this model and The adsorbed experimental quantities $Q_{e,exp}$ are closer.

TABLE 3

ADSORPTION KINETICS CONSTANTS OF RR-23 ON CLSh AND THE BCCLSh (T=25±1°C, M=50MG, C_O=5 mg.L^{-1}; STIRRING =200 rpm AND pH=7±0.5)

models	The constants	CLSh	BCCLSh
Pseudo-1st-order	R^2	**0.946**	**0.853**
	K_1(ml.min^{-1})	0.077	0.058
	$Q_{e,cal}$ (mg.g^{-1})	31.63	10.06
	$Q_{e,exp}$ (mg.g^{-1})	35.33	49.75
Pseudo-2nd-order	R^2	**0.997**	**0.999**
	K_2(g.mg^{-1}.min^{-1})	0.004	0.007
	$Q_{e,cal}$ (mg.g^{-1})	38.46	52.63
	$Q_{e,exp}$ (mg.g^{-1})	35.33	49.75
Elovich model	R^2	**0.851**	**0.713**
	α (mg.g^{-1}.min^{-1})	20.873	830.605
	β (g.mg^{-1})	0.1586	0.1893
Intraparticule diffusion model	R^2	**0.709**	**0.553**
	K_i (mg.g^{-1}.$min^{0.5}$	1.761	1.423
	C (mg.g^{-1})	18.99	36.71

3.3 Adsorption isotherms

The adsorption isotherm indicates how the molecules are distributed between the liquid phase and the solid phase when the adsorption reaches equilibrium. It is well known that, the modeling of adsorption isotherms is the first objective to be achieved in any scientific investigation, since it serves as a rational mathematical tool allowing passing from the experimental phase of laboratory to that of conception at the scale of prototype. The variation in the amount (Q_e) of the CLSh and the BCCLSh adsorbed RR-23 dye as a function of the equilibrium concentration (C_e) is shown in Figure 11 and figure 12. On the other hand, several models are cited in the literature to describe Experimental data from adsorption isotherms. In this study, the isotherms models studied are the Lungmuir model, Freundlich model, Temkin model and the Dubinin-Radushkevich model.

The most frequently established model for the study of adsorption isotherms is chosen as a function of the correlation factor. The model of Lungmuir which is a correlation factor (R^2 = 0.996) and the maximum adsorbed amount by the CLSh is equal to 90.91mg.g^{-1}, whereas the model applied in the adsorption of RR-23 on the BCCLSh is the model of Lungmuir and Freundlich with a correlation factor (R^2=0.984) is the adsorbed amount equal to 354.82mg.g^{-1}. The isothermal constants obtained by linearization of the various models considered are summarized in Table 4, while the

correlation between the experimental values and those predicted by the best model is illustrated in figure 11, 12, 13 and figure 14.

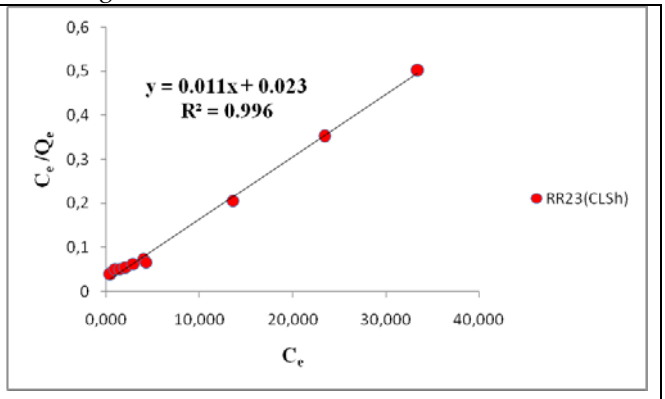

Fig.11. *The Lungmuir Isotherms for the adsorption of RR-23 on the CLSh (T =25 ±1°C, m=50 mg, stirring = 200 rpm and pH =7±0.5)*

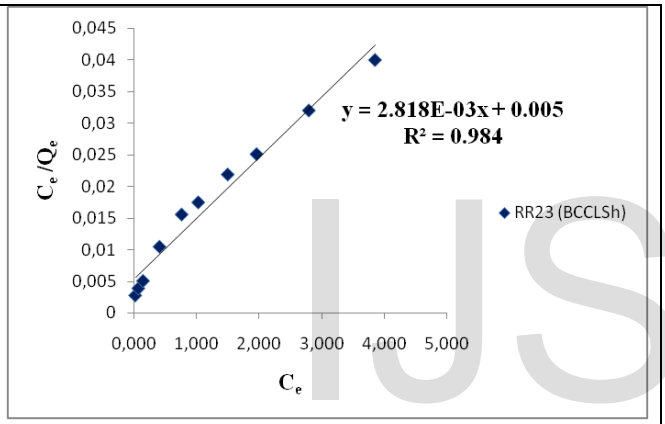

Fig.12. *The Lungmuir Isotherms for the adsorption of RR-23 on the BCCLSh (T =25 ±1°C, m=50 mg, stirring = 200 rpm and pH =7±0.5)*

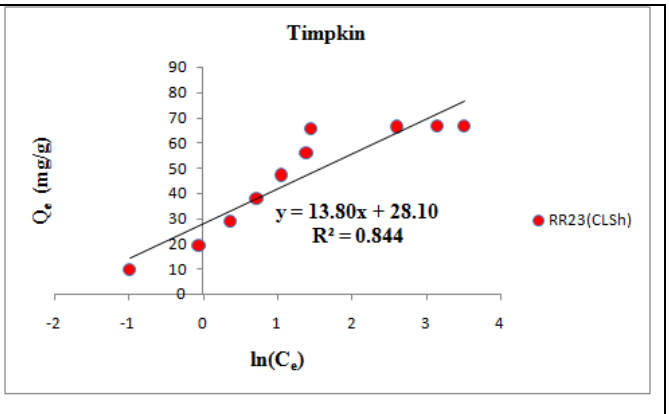

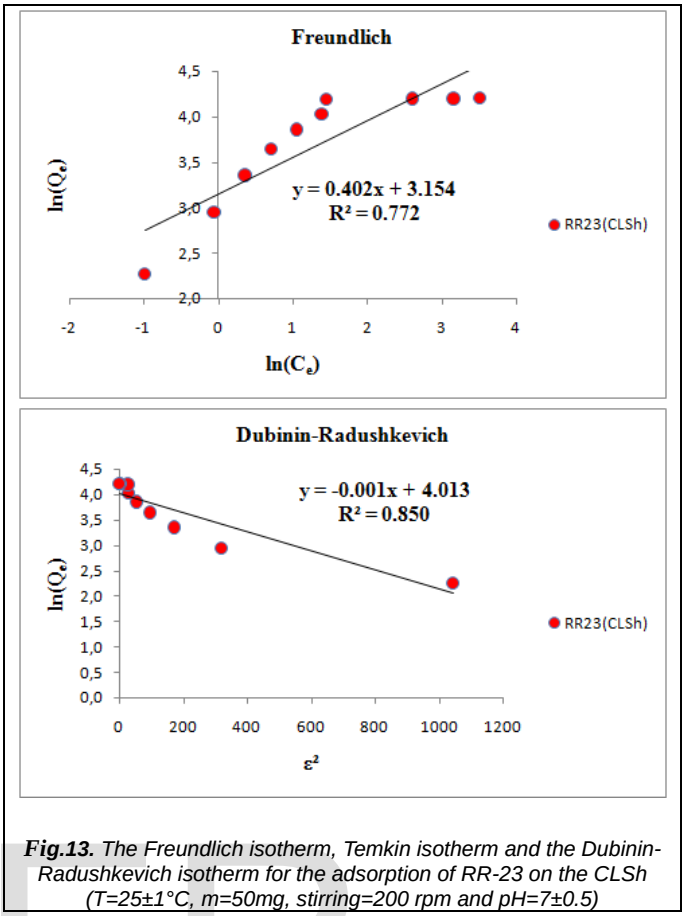

Fig.13. *The Freundlich isotherm, Temkin isotherm and the Dubinin-Radushkevich isotherm for the adsorption of RR-23 on the CLSh (T=25±1°C, m=50mg, stirring=200 rpm and pH=7±0.5)*

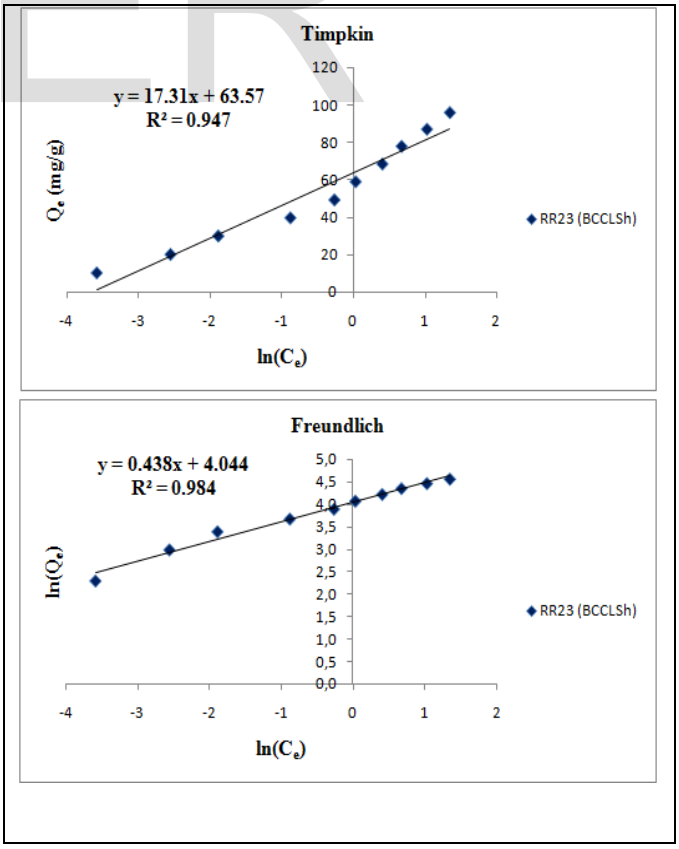

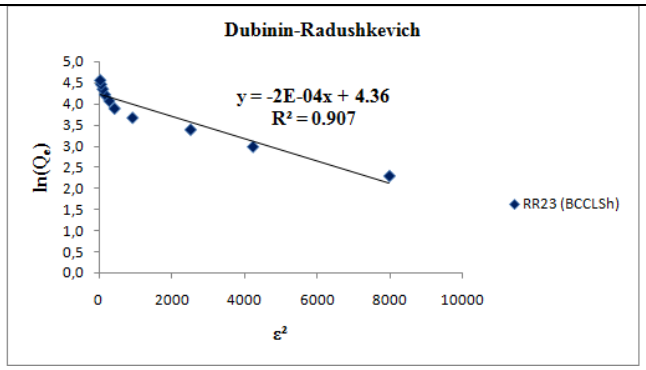

Fig.14. *The Freundlich isotherm, Temkin isotherm and the Dubinin-Radushkevich isotherm for the adsorption of RR-23 on the BCCLSh (T=25 ±1°C, m=50mg, stirring = 200 rpm and pH=7±0.5)*

TABLE 4
CONSTANT ADSORPTION ISOTHERMS OF RR-23 ON CLSh AND BCCLSh (T = 25 ± 1 ° C, M=50 mg, AGITATION=200 rpm AND pH =7±0.5)

isotherms	parameters	CLSh	BCCLSh
Lungmuir Isotherm	**R^2**	**0.996**	**0.984**
	R_L	0.0205 - 0.1736	0.0174 - 0.1508
	K_L *(L.mg^{-1})*	0.476	0.563
	Q_m *(mg.g^{-1})*	90.91	354.82
Freundlich Isotherm	**R^2**	**0.772**	**0.984**
	K_F	23.429	57.054
	n	2.487	2.283
Temkin Isotherm	**R^2**	**0.844**	**0.947**
	K_T *(L.g^{-1})*	7.662	39.348
	B_1 *(J.mol^{-1})*	13.80	17.31
	b	179.45	143.06
Dubinin-Radushkevich Isotherm	**R^2**	**0.850**	**0.8907**
	K_{ad} *(mol^2.Kj^{-2})*	0.001	0.0002
	E*(Kj.mol^{-1})*	23.36	50
	Q_m *(mg.g^{-1})*	55.312	69.131

3.4 Adsorption thermodynamics studies

The thermodynamic parameters such as the Gibbs free energy change (ΔG^o), enthalpy (ΔH^o) and entropy (ΔS^o) were calculated using the following equations [22]:

$$K = \frac{Q_e}{C_e} \qquad \text{(eq.22)}$$

The value of ΔG^o can be determined from the following equation

$$\Delta G^o = -RT \ln K \quad \text{(eq.23)}$$

Where K is the thermodynamic equilibrium constant
The effect of temperature on thermodynamic constant is determined by

$$\frac{d(LnK)}{dt} = \frac{\Delta H^0}{RT^2} \quad \text{(eq.24)}$$

Integrating and rearranging equation (eq.24) we get

$$Ln\,(K) = \frac{\Delta S_0}{R} - \frac{\Delta H_0}{RT} \quad \text{(eq.25)}$$

And Gibbs free energy is also given by

$$\Delta G^o = \Delta H^o - T\Delta S^o \quad \text{(eq.26)}$$

The ΔH^o and ΔS^o values were calculated from the slope and intercept of linear plot of lnK versus 1/T Figure 15. Such parameters reflect the feasibility and spontaneous nature of the process [23]. Experiments were carried out using 50 mg.L^{-1} dye solutions with 50 mg of CLSh or BCCLSh for 90 minutes at different temperatures. The apparent equilibrium constant K of the adsorption is calculated by equation (eq.22). The free energy of Gibbs of the adsorption $\Delta G°$ is calculated from the following equation (eq.24), the relationship between the K and the temperature is given by the Van't Hoff equation [3], enthalpy and entropy can be obtained from the slope and the interception of Van't Hoff plot of Ln K with respect to 1/T which are shown in Figures 15. The results summarize the thermodynamic parameters such as $\Delta H°$, $\Delta S°$ and $\Delta G°$ for the RR23 dye are summarized in Table 5.

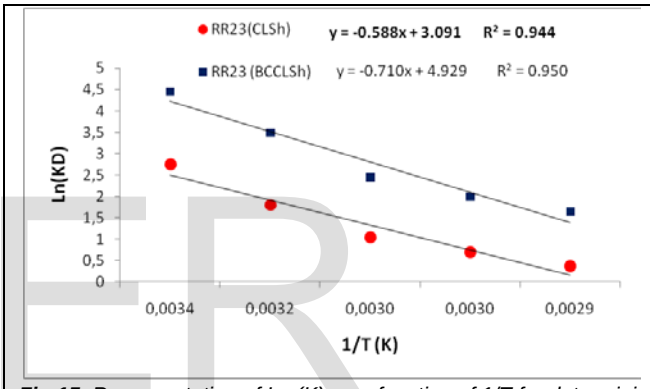

Fig.15. *Representation of Ln (K) as a function of 1/T for determining the thermodynamic parameters of component RR23 dye on the CLSh and BCCLSh (m=50 mg, C_o=50 mg.L^{-1}, pH=7±0.5, Stirring=200 rpm)*

TABLE 5
THERMODYNAMIC PARAMETERS ΔH°, ΔS° AND ΔG° RELATING TO THE COMPONENT RR23, ADSORPTION ON THE CLSh AND BCCLSh (M=50 mg, C_O=50 mg.L^{-1}, pH=7± 0.5, STIRRING=200 rpm)

parameters		CLSh	BCCLSh
ΔH° (J.mol^{-1})		4.8863	5.900
ΔS° (J.mol^{-1}.K^{-1})		25.686	40.960
ΔG° (kJ.mol^{-1})	T= 298°K	-7.649	-12.200
	T= 308°K	-7.906	-12.610
	T= 328°K	-8.420	-13.429
	T= 338°K	-8.677	-13.839
	T= 348°K	-8.934	-14.248

The $\Delta S°$ of the adsorbed RR23 is negative, which implies that the adsorption is carried out with an order increase in the solid solution interface and that the

distribution order of the component molecules on the adsorbent CLSh or BCCLSh is high compared to that in the solution. Same observation for ΔH°, which is also positive, which means that our adsorption process is endothermic [24]. The enthalpy of chmisorption is between 40 and 120 KJ.mol^{-1} and for physisorption; it is less than 40kJ.mol^{-1}. The thermodynamic results show that the nature of the adsorption is physical, whereas for CLSh and BCCLSh, the nature of the adsorption is physical [25,26], which is confirmed by the validity of the pseudo-second order kinetics which introduces the probability of existence of a valence force by the sharing or exchange of electrons between the adsorbent and the adsorbate. Physical and chemical adsorption exists during the fixation of the dye in the micropores and also in the nanopores.

According to the values of Table 5, the ΔG ° decreases with the increase of the temperature of the solution, this means that the adsorption becomes very hard and disadvantaged by a higher temperature. The redistribution of energy between the adsorbent and the adsorbate is fairly clear due to the positive values of ΔG° [27, 28], with an increase in the randomness at the solid solution interface during the RR23 dye fixing process, on the CLSh or BCCLSh, from these negative values of ΔG ° it can be said that the adsorption of the treated components is spontaneous.

4 Conclusion

The Cistus ladaniferus plant used as a source of biomaterials the production of shells and biochar this last is synthesized by the pyrolysis process was characterized by infrared spectroscopy (FT-IR), scanning electron microscope (SEM), Energy Dispersive X-rays Spectroscopy (EDXS) and Wavelength Dispersive X-ray Fluorescence Spectrometry (WDXFS). These materials are used as bio-adsorbents for the removal of the RR-23 dye.

The adsorption kinetics was explained using a pseudo-second order model. The Langmuir type II isotherm and the Freundlich model are the two most widely applied models in dye adsorption on BCCLSh and type I adapted for CLSh which was consistent with the equilibrium data of 'adsorption. The adsorption capacity for the CLSh and the BCCLSh in terms of the absorption capacity of the RR-23 dye reaches a value of 90.91mg.g^{-1} for CLSh and 354.823mg.g^{-1} for BCCLSh at the initial pH of 7±0.5, a temperature of 298±1K and the mass of adsorbent equal to 50 mg. The results indicate that the CLSh adsorbent or BCCLSh can be used as an effective and promising bioadsorbant for the removal of industrial dyes, for example in our study the red reactive 23 was used in aqueous solutions.

References

1. H. El Farissi, R. Lakhmiri, H. El Fargani, A. Albourine, and M. Safi, "Valorisation of a Forest Waste (Cistus Seeds) for the Production of Bio-Oils," *JMES*, vol. 8, no. 2, pp. 628–635, 2017.
2. H. El Farissi, R. Lakhmiri, H. El Fargani, A. Albourine, and M. Safi, "Production of Bio-Oil from Cistus Ladanifer Shell by Fixed-Bed Pyrolysis,"*IJENS-IJET,* vol. 17, no. 4, 2017.
3. P. B. Venkat S. V. Mane , "Studies on the adsorption of Brilliant Green dye from aqueous solution onto low-cost NaOH treated saw dust," *Desalination*, vol. 273, no. 2–3, pp. 321–329, 2011.
4. M. Ghaedi, A. Ansari, F. Bahari, A. M. Ghaedi, and A. Vafaei, "A hybrid artificial neural network and particle swarm optimization for prediction of removal of hazardous dye brilliant green from ... Spectrochimica Acta Part A□: Molecular and," *Spectrochim. ACTA PART A Mol. Biomol. Spectrosc.*, vol. 137, no. September 2014, pp. 1004–1015, 2015.
5. S. Ertugrul, N. O. San, and G. Donmez, "Treatment of dye (Remazol Blue) and heavy metals using yeast cells with the purpose of managing polluted textile wastewaters," *Ecol. Eng.*, vol. 35, no. 1, pp. 128–134, 2009.
6. E. Daneshvar, M. Kousha, M. Jokar, N. Koutahzadeh, and E. Guibal, "Acidic dye biosorption onto marine brown macroalgae: Isotherms, kinetic and thermodynamic studies," *Chem. Eng. J.*, vol. 204–205, pp. 225–234, 2012.
7. H. El Farissi, R.Lakhmiri, A.Albourine, M. Safi and O. Cherkaoui, "Removal of RR-23 dye from industrial textile wastewater by adsorption on cistus ladaniferus seeds and their biochar," *Journal of Environment and Earth Science.*, Vol.7, No.11, pp. 105–118, 2017.
8. H. El Fargani, R. Lakhmiri, A. Albourine, O. Cherkaoui, and M. Safi, "Valorization of shrimp co- products ' Pandalus borealis ': Chitosan production and its use in adsorption of industrial dyes," vol. 7, no. 4, pp. 1334–1346, 2016.
9. N. Mohammad, R. Salehi, M. Arami, and H. Bahrami, "Dye removal from colored textile wastewater using chitosan in binary systems," *DES*, vol. 267, no. 1, pp. 64–72, 2011.
10. H. El Fargani, R. Lakhmiri, H. El Farissi, A. Albourine, M. Safi, and O. Cherkaoui, "Removal of anionic dyes by silica-chitosan composite in single and binary systems□: Valorization of shrimp co- product ' Crangon - Crangon ' and ' Pandalus Borealis ," *iiste-JCMR*, vol. 8, no. 2, pp. 724–739, 2017.
11. K. A. Publishers and B. Centre, "Citation review of Lagergren kinetic rate equation on adsorption reactions," vol. 59, no. 1, pp. 171–177, 2004.
12. G. Mckay, Y. S. Ho, and G. Mckay, "Pseudo-Second Order Model for Sorption Process," no. September 2017, 1999.
13. S.H. Chien & W.R. Clayton, 1980. Application of Elovichequation to the kinetics of phosphate release and sorption in soils. *SoilSci. Soc. Am. J .*, 44 , 265-268.," p. 1980, 1980.
14. K. Urano, and T. Hirotaka, 'Process Development for Removal and Recovery of Phosphorus from Wastewater by a New Adsorbent. 2. Adsorption Rates and Breakthrough Curves' Ind. Eng. Chem. Res. 30 (1991) 1897-189," vol. 30, p. 1991, 1991.
15. I. Langmuir, *Am. J., Chem. Soc.*, 40 (1918) 1361–1403." .
16. M. Ghasemi, S. Mashhadi, M. Asif, I. Tyagi, S. Agarwal, and V. Kumar, "Microwave-assisted synthesis of tetraethylenepentamine functionalized activated carbon with high adsorption capacity for Malachite green dye," *J. Mol. Liq.*, 2015.

17. K. Sujoy Das, Jayati Bhowal, R. Akhil Das, and K. Arun Guha "Adsorption Behavior of Rhodamine B on Rhizopus o ryzae Biomass," *Langmuir*, vol. 22, no. 17, pp. 7265–7272, 2006.
18. M. Laabd, H. Chafai, A. Essekri, M. Elamine, R. Lakhmiri, and A. Albourine, "Single and multi-component adsorption of aromatic acids using an eco-friendly polyaniline-based biocomposite," *Sustainable Materials and Technologies* Vol. 12, no.1, 2017, pp. 35-43
19. M. F. Maryam Ghasemi, Mohammad zeinaly khosroshahy, Arash Bavand ab- basabadi, Nahid Ghasemi, Hamedreza Javadian, "Microwave-assisted functionalization of Rosa Canina-Lfruits activated carbon with tetraethylenepentamine and its adsorption behavior toward Ni (II) in aqueous solution: Kinetic, equilibrium and thermodynamic studies," *Powder Technol.*, no. Ii, 2014.
20. M. Ghasemi, H. Javadian, N. Ghasemi, S. Agarwal, and V. Kumar, "Microporous nanocrystalline NaA zeolite prepared by microwave assisted hydrothermal method and determination of kinetic , isotherm and thermodynamic parameters of the batch sorption of Ni(II)," *J. Mol. Liq.*, vol. 215, pp. 161–169, 2016.
21. E. R. V. William J. Weber, Alexandra Navrotsky, Sergey Stefanovsky, "Materials Science of High-Level Nuclear Waste Immobilization." p. vol 34. no 1, 46-53, 2011.
22. G. P. Jin, X. L. Wang, Y. Fu, and Y. Do, "Preparation of tetraoxalyl ethylenediamine melamine resin grafted-carbon fibers for nano-nickel recovery from spent electroless nickel plating baths," *Chem. Eng. J.*, vol. 203, pp. 440–446, 2012.
23. B. Mahjoub, M. C. Ncibi, and M. Seffen, "Posidonia OceaniAdsorption d'un Colorant Textile R??actif sur un Biosorbant Non-Conventionnel: Les Fibres deca (L.) Delile," *Can. J. Chem. Eng.*, vol. 86, no. 1, pp. 23–29, 2008.
24. H. El Fargani. L. Rajae, H. EL Farissi, A. Albourine, and M. Safi, "Modified Chitosan Immobilized on Modified Sand for Industrial Wastewater Treatment in Multicomponent Sorption□: Shrimp Biowaste Processing," *JMES*, vol. 9, no. 4, pp. 20–42, 2017.
25. S. Netpradit, P. Thiravetyan, and S. Towprayoon, "Adsorption of three azo reactive dyes by metal hydroxide sludge: Effect of temperature, pH, and electrolytes," *J. Colloid Interface Sci.*, vol. 270, no. 2, pp. 255–261, 2004.
26. N. Barka, S. Qourzal, A. Assabbane, A. Nounah, and Y. Ait-Ichou, "Removal of Reactive Yellow 84 from aqueous solutions by adsorption onto hydroxyapatite," *J. Saudi Chem. Soc.*, vol. 15, no. 3, pp. 263–267, 2011.
27. R. Aravindhan, N. N. Fathima, J. R. Rao, and B. U. Nair, "Equilibrium and thermodynamic studies on the removal of basic black dye using calcium alginate beads," *Colloids Surfaces A Physicochem. Eng. Asp.*, vol. 299, no. 1–3, pp. 232–238, 2007.
28. M. Ait Haki, M. Laabd, H. Chafai, H. Kabli, M. Ez-zahery, M. Bazzaoui, R. Lakhmiri & A. Albourine, "Comparative Adsorption of Nitrate Ions on the Polypyrrole and Polyaniline From Aqueous Solution," no. May, 2016.